Feature Extraction of Contaminated Oil Signal Based on HHT

Ge, Liu
School of Environmental Engineering, North China Institute of Science and Technology, Hebei, 065201, P.R. CHINA

Bin, Chen*[+]
School of Mechanical & Electrical, Hebei Key Laboratory of Safety Monitoring of Mining Equipment, North China Institute of Science and Technology, Hebei, 065201, P.R. CHINA

Deng, Yangqin
Engineering Research Centre for Waste Oil Recovery Technology and Equipment, Chongqing Technology and Business University, Chongqing, 400067, P.R. CHINA

ABSTRACT: *The movement state of contaminated oil in the pipeline is of great significance to the safe operation of oil-using equipment. The dynamic motion characteristics of the oil can be characterized by signals. However, the pressure signal of the oil is time-varying and complex; hence it is a typically non-stationary nonlinear signal. Therefore, the traditional linear analysis method used for the analysis of the oil signal is not suitable. For this reason, the Hilbert-Huang Transform (HHT) method is used to process and analyze the differential pressure signals of oils with different degrees of pollution, to obtain the characteristic frequencies of oil pressure signals, to explore the intrinsic connection of the characteristic frequencies and oils with different degrees of pollution, and to reveal the dynamic movement characteristics of oil in the pipeline. The results show that the characteristic frequencies corresponding to the five groups of oil samples with a pollution degree of 17/12,18/12,19/13,19/13,20/16 (ISO4406 standard) are 20.29 Hz, 10.22 Hz, 6.94 Hz, 17.01 Hz, and 6.81 Hz, respectively; Each Intrinsic Mode Function (IMF) component of the oil signal has obvious frequency modulation characteristics; As the pollution degree increases, the oil frequency of the IMF2-4 component mainly shifts toward the middle of the interval, and the oil frequency of the IMF5-7 component mainly shifts toward the direction of 5.00 Hz, 3.00 Hz, and 1.60 Hz respectively.*

KEYWORDS: *Differential pressure signal; Hilbert-Huang transform; Contaminated oil; Pressure signal; The characteristic frequency; The pollution degree.*

INTRODUCTION

The oil medium is a vital part of the equipment system; it has many functions such as sealing, anti-corrosion, cooling, lubrication. However, if the pressure in the equipment system changes, the physical and chemical

***** *To whom correspondence should be addressed.*
+ *E-mail: hustchb@ncist.edu.cn*
1021-9986/2022/10/3445-3457 13/$/6.03

properties and flow properties of the oil will change, which will cause the system to malfunction and affect the efficiency of the equipment during usage. Therefore, it is of great significance to analyze the movement characteristics of the oil in the pipeline and to grasp the changes in the oil under different pollution degrees [1]. Secondly, the pollution degree of the oil will affect the fluid flow, causing it to produce vortices of different sizes. The development of the vortex will cause the oil to pulsate. Therefore, the oil pollution degree can be assessed by the oil pressure [2].

The dynamic motion characteristics of the oil can be characterized by signals. However, because the pressure signal of the oil is time-varying and complex, it is a typical non-stationary nonlinear signal. Therefore, the traditional linear analysis method is not suitable for the analysis of the oil signal. Recently, the methods of processing such signals mainly include wavelet transform [3-5], wavelet packet decomposition [6, 7], variational mode decomposition [8-10], mutual Correlation analysis [11, 12], short-time Fourier transform [13, 14] and HHT [15-17], etc. HHT method is an emerging processing technology, which is not limited by Fourier analysis. It can be adaptively decomposed from the characteristics of the signal itself while depicting the time spectrum and amplitude of the signal spectrum. Therefore, in recent years, the HHT method has been widely used to process non-stationary nonlinear signals. In the analysis of fluid dynamic characteristics, the fluid flow pattern is mainly identified by using the energy change law of the IMF component. Haifeng *Ji et al.* [18] used empirical mode decomposition to identify the flow pattern of gas-liquid two-phase flow in microchannels with the extracted characteristic parameters and IMF energy as the input parameters of the least squares support vector machine. The experimental results show that the method has high accuracy in identifying the four flow patterns of annular flow, bubble flow, slug flow, and stratified flow. *Li Weiling et al.* [19] analyzed the relationship between the Empirical Mode Decomposition (EMD) energy entropy and the flow state transition in the gas-liquid-solid three-phase bubble column. It was found that when the flow state changes, the EMD energy entropy of the system will change, and the two transition points and the three main flow states of uniform flow, transition flow, and heterogeneous flow in the three-phase bubble tower can be observed obviously. In addition to using IMF energy as a characteristic value, frequency bands can also be divided according to the frequency characteristics of the IMF component, and the energy ratio of each frequency band is used as a characteristic value to characterize the dynamic change of the fluid. *Peng Lu et al.*[20] analyzed the pressure fluctuation signals under three flow modes of stratified flow, dune flow, and plug flow in the high-pressure pneumatic conveying system. They used the energy change of the frequency band as an index to identify the flow pattern of compressed gas-solid flow and obtained the law between energy change and flow pattern change. *Li Xiaolu et al.* [21] judged the fluid flow pattern according to the change law of the energy ratio of each frequency band under different flow patterns and obtained that the brake fluid in the hydraulic brake line of the car was a bubbly flow.

The above studies have achieved good experimental results, effectively proving the effectiveness of using the HHT method to analyze nonlinear non-stationary signals, so this research uses the HHT method to process and analyze the oil pressure signal. The characteristic frequency of oils with different pollution degrees is extracted, and the internal relationship between oil pollution and oil signals with different pollution degrees is discussed.

EXPERIMENTAL SECTION

Experimental setup

The experimental device mainly includes two parts: the oil circuit device and the oil pressure signal acquisition system. The oil circuit device consists of an oil source, an oil inlet pipe, a flow sensor, an oil inlet connection block, a test pipe, an outlet connection block, a control valve, and an oil outlet pipe is shown in Fig. 1. The high precision pressure sensor1 and pressure sensor2 are set above the oil inlet connecting block and the oil return connecting block, respectively. The diameter of the oil inlet pipe and the oil return pipe is 24mm. The experimental pipeline is set as a rectangular parallelepiped with a cross-section of 0.04 × 0.04m and a length of 0.50m. The front wall surface and the top surface of the pipeline are made of transparent tempered glass, and the bottom surface and rear wall surface are made of steel plates.

The oil pressure signal acquisition system mainly includes three parts: import and export sensors, data

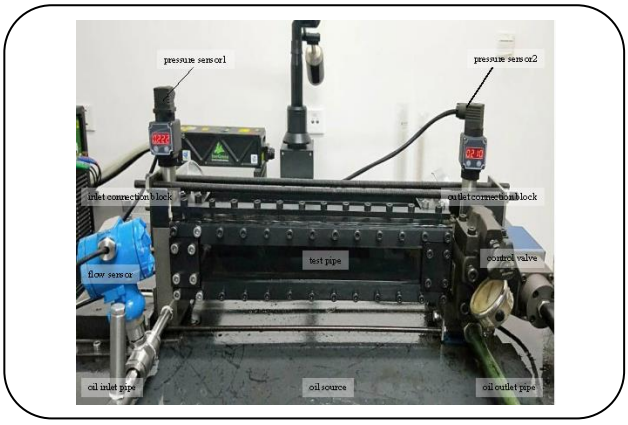

Fig. 1: The diagram of the oil circuit device.

acquisition card, and LabVIEW software. Among them, the inlet and outlet pressure sensors are YP-01S type sensors; their range is -0.10-2.00MPa. The power supply range is 12-36V, and the output range is 0-5V; The data acquisition card uses the NI PXI-6133 acquisition card produced by the American NI company. The acquisition card is a synchronous sampling multifunctional data acquisition device, which can provide 8 analog input channels (14 bits, each channel up to 2.50 MS/s rate), 8 digital I / O lines, and 2 24-bit counter and triggers. Import and export sensors convert the collected oil pressure signals into electrical signals and transmit them to the data acquisition card. The acquisition card converts the oil pressure signal into a digital signal and transmits it to the LabVIEW software on the computer for real-time display and storage.

Method for collecting oil pressure signal

This paper uses LabVIEW software to compile the oil pressure signal acquisition system. The front panel mainly includes the parameter setting area and waveform display area (original waveform display area and filter display area). The parameter setting area specifically sets the acquisition parameters, such as the sampling rate of 20000 Hz, the number of samples of 1000, the continuous sampling mode, and there are buttons for data saving, picture saving, filter, etc. The waveform display area mainly displays the changes in the inlet pressure signal, outlet pressure signal, and flow signal of the pipeline oil over time and the filtering situation in real-time.

The preparation process of the contaminated oil is shown in Fig. 2. The experimental oil is selected as 25 # transformer oil. In order to prevent the particulate matter mixed in the factory oil during production and transportation from interfering with the experiment, the transformer oil was vacuum filtered to obtain the initial oil. Copper powder (10.00g) and silica powder (10.00g) are used as particulate contaminants, and it is mixed evenly with 500.00 mL of initial oil by shaking with an ultrasonic oscillator for at least 2 hours to prepare a highly contaminated oil. After the high-pollution oil is mixed evenly, the large particles in the oil are filtered by neutral filter paper. A high concentration of contaminated oil is then added in proportion to the tank and run in the pipeline for at least two hours. Because the oil source is set with a filter precision of 25μm, according to the ISO4406 standard, the different pollution levels of oil are classified according to the number of particles 5μm particle size and 15 μm particle size. After the HACH 8000A pollution tester (HACH Company) test, 5 sets of contaminated oil samples were obtained. The pollution level and particle number of each oil sample group obtained are shown in Table 1. The prepared oil is fed into the experimental pipeline through the hydraulic motor blade pump, first through the pipeline development section into the test section, then through the tail section into the oil tank, and the cycle is formed.

Put the prepared contaminated oil into the experimental pipeline and circulate for 30 minutes. After the pressure value displayed by the pressure sensor changes to relatively stable, start collecting the oil signal. The time is about 160 s.

RESULTS AND DISCUSSION

Pretreatment of oil signal

There is a lot of noise interference in the inlet and outlet pressure signals of the oil. Especially the oil inlet pressure signal has many signal glitches, most of which is due to the influence of noise interference. Therefore, first, use the inlet pressure signal to subtract the outlet pressure signal to obtain the differential pressure signal to eliminate the vibration of the pipeline itself. Secondly, wavelet analysis is used to filter the obtained pressure difference signal. We choose db 5 as the wavelet base, and the number of decomposition layers is four. The resulting filtered signal and original signal are shown in Fig. 3.

Table 1: The number of particles of different sizes contained in each group (pieces / mL).

Number of groups	Pollution degree	5um particles	15um particles
1	17/12	1147.33	28.04
2	18/12	1580.75	40.25
3	19/13	2567.50	73.58
4	19/13	3088.11	82.17
5	20/16	5187.00	406.42

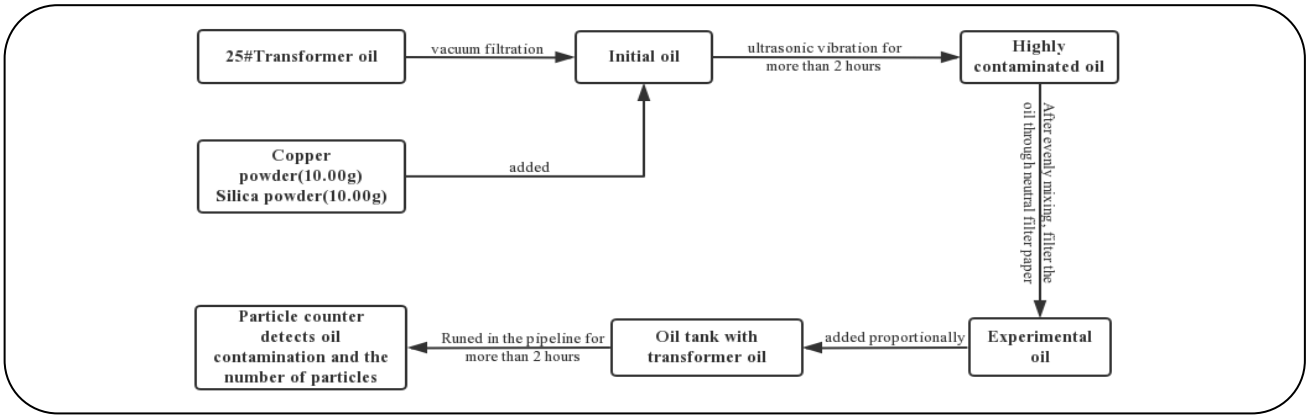

Fig. 2: Flow chart of contaminated oil preparation.

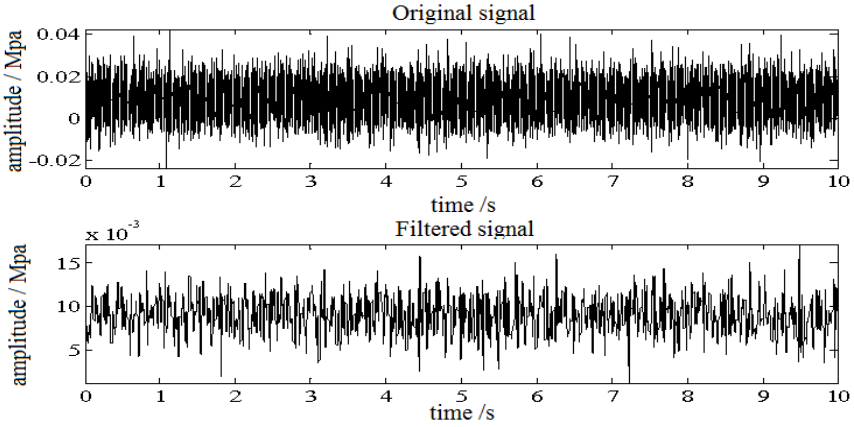

Fig. 3: Original pressure difference signal and filtered signal.

By observing Fig. 3, it can be found that wavelet decomposition filters out many complex high-frequency components in the original signal, and the obvious shock component in the original signal still exists. Therefore, the use of Hilbert-Huang transforms to process the filtered signal is more conducive to subsequent analysis.

IMF component

In practical applications, the IMF components decomposed by EMD usually have modal aliasing and end effects. They will cause some components to fail to obtain the correct physical meaning, which will increase the difficulty of feature signal extraction and affect the subsequent analysis. Therefore, to avoid such problems, the noise-assisted Ensemble Empirical Mode Decomposition (EEMD) method based on EMD decomposition is used to process and analyze the oil signal. The differential pressure signal of the oil is decomposed by EEMD to produce 14 IMF components. Due to the five sets of pollution degrees, the impact components of IMF 1

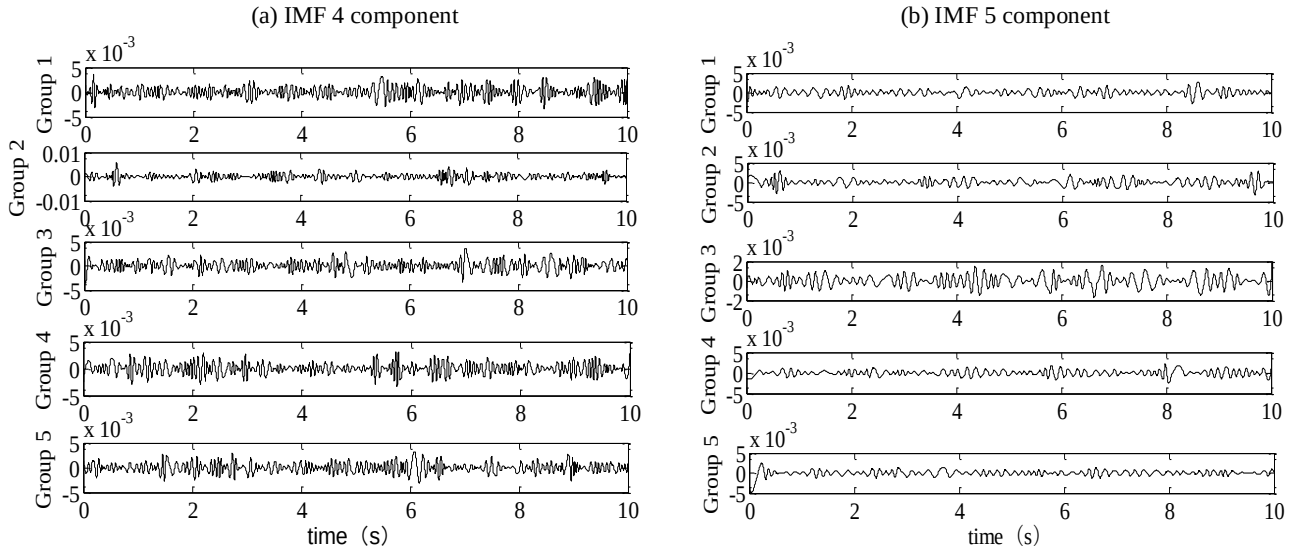

Fig. 4: IMF 4-5 components of oil with different pollution degrees.

complex. However, the impact components of the three components of IMF 4-5 are more obvious. When decomposed to the IMF 6 component, the impact component is significantly reduced, and its change is not obvious. The development trend of components after IMF 7 is stable. Therefore, the IMF 4-5 components in each group of pollution degrees were extracted for analysis, as shown in Fig. 4. The horizontal axis represents time, and the vertical axis represents signal amplitude.

It can be seen from Fig. 4(a) that at about 0.1 s of the IMF 4 component, all five groups of contaminated oil produced impact components, with amplitudes of 3.49×10^{-3}, 1.88×10^{-3}, 1.97×10^{-3}, 1.50×10^{-3} and 1.48×10^{-3}, respectively. The amplitude of the impact component generated by the Group 1 is the largest, almost twice that of the other four groups. It is shown that at 0.1 s, the effect of particulate matter on the oils is most obvious in Group 1, and the impact component produced at this time may also be the characteristic component of Group 1; Secondly, as the pollution degree increases, the amplitude of the impact component generated at this time tends to decrease gradually. In about 0.5 s, the amplitudes of the impact components generated by the five groups of oils are 1.55×10^{-3}, 5.85×10^{-3}, 1.28×10^{-3}, 1.98×10^{-3} 和 0.88×10^{-3}, respectively. Group 1, Group 3, and Group 4 are relatively similar in magnitude. Group 5 is relatively small, which is close to half of Group 4, but Group 2 has the largest amplitude, almost 3-5 times the pollution degree of the other four groups. It shows that at 0.5 s, the influence of particles on the oil is most obvious in Group 2. The impact component generated at this time is the characteristic component of Group 2. At around 0.9 s, the impact components were generated in Groups 1 and 3-5, and the amplitudes were relatively close, respectively 1.41×10^{-3}、1.52×10^{-3}, 2.73×10^{-3}, 1.16×10^{-3}. The impact component of Group 2 is not obvious, but Group 4 has the largest amplitude, which is about twice the amplitude of other groups. It shows that the influence of particles on the oil is enhanced in Group 4. That is, 0.9 s is the characteristic of Group 4. At around 2.7 s, the magnitudes of the pollution impact components in Group 1 and 2 were 1.24×10^{-3} and 1.43×10^{-3}, respectively. The impact components of Group 3 and 4 currently are not obvious. However, when the pollution degree of the oil increases to Group 5, the amplitude of the impact component is 2.92×10^{-3}, and the effect of particulate matter on the oil is significantly enhanced in Group 5, which also shows that it is the characteristic of Group 5 at 2.7 s. Around 4.8 s, the amplitude of the impact component generated by Group 4 is 0.80×10^{-3}, which is significantly lower than the amplitude of the other groups, about one-third of them. It shows that the influence of particles on the oil is attenuated in Group 4, which is the characteristic moment of the pollution degree of Group 4 at 4.8 s. At 6.7 s and 7.0 s, the amplitude of the impact components of Group 5 of pollution degrees were 0.82×10^{-3} and 0.76×10^{-3}, which

were significantly lower than those of the other groups, indicating that 6.7 s and 7.0 s were the characteristic moments of Group 5. At about 9.5 s, the amplitude of the impact component of Group 3 of pollution degree is 0.92×10^{-3}, which is significantly lower than the amplitude of the impact component of the other groups, indicating that the impact of particles on the oil is the weakest in Group 3. It also shows that 9.5 s is the characteristic time of Group 3. It can be seen that with the increase of the number of particles, the maximum impact time of oil flow pressure presents a gradually increasing trend. This is because with the increase of particle concentration in the oil, particle inertia increases the average flow velocity in the near-wall region, and the thickness of the turbulent viscosity bottom decreases and the flow velocity gradient increases [22], which leads to the gradual delay of the pressure pulsation time of the oil flow.

In about 1.5 s, the amplitudes of the impact components generated by the five groups of oils with pollution degrees are 0.94×10^{-3}、0.92×10^{-3}、2.25×10^{-3}、1.78×10^{-3}、2.62×10^{-3}, respectively. The amplitude of Group 1 and Group 2 is significantly lower than that of Groups 3-5, indicating that the impact of particulate matter on the pollution degree of Groups 1 and 2 was weakened around 1.5 s. Around 3.5 s, the amplitudes of Groups 3 and 4 were significantly lower than the other groups, indicating that the effect of particulate matter on the oil has weakened in Groups 3 and 4. However, in about 4.5 s, the amplitudes of Group 2 and Group 3 were significantly higher than those of the other three groups, indicating that the influence of particulate matter on the oil in Group 2 and Group 3 was enhanced. At 5.7 s, the amplitudes of Groups 4 and 5 have increased compared with the first three groups, indicating that the impact of particulate matter on the oil has increased under the pollution of Groups 4 and 5. At about 6.1 s, the impact components of Groups 1 and 5 increased in amplitude compared to the other three groups, indicating that the impact of particulates on the oil increased under the pollution levels of Groups 1 and 5. As can be seen at the same time, due to the oil pulsation amplitude with the increase of particle concentration, the periodic change, that illustrate the impact of particles on the oil pressure in the oil in Group 3 showed a trend of decrease when the particle concentration, when the particle concentration more than Group 3 of particle concentration, the oil pressure fluctuation and showed a trend of increase; this is because with the increase of particle concentration, the viscous shear force of oil increases and the pulsation degree of oil decreases. When the particle concentration reaches a certain level, the particle settlement makes the wall surface form a rough wall surface, it enhances the turbulence burst behavior in the near-wall area, which leads to the increase of oil pulsation.

It can be seen from Fig. 4 (b) that around 0.2 s in the IMF 5 component, there is a significant impact component in the pollution degree of Group 5. However, the impact component of the pollution degree in groups 1-4 is not obvious. It shows that when the pollution degree is increased to Group 5, the impact component is enhanced at 0.2 s, a characteristic moment of Group 5. Around 0.6 s, the impact component of Group 2 is significantly enhanced compared to the other four groups, with an amplitude of 3.03×10^{-3}, indicating that 0.6 s is a characteristic moment of Group 2. At about 1.3 s, the amplitude of the impact components of the first and fifth groups is more obvious, and the impact components of Groups 2-4 are attenuated. At around 1.9 s, the amplitudes of Group 1 and Group 2 are more obvious. With the increase in pollution, the impact components of Groups 3-5 were significantly weakened. At 4.3 s, there is a significant impact component in Groups 1-4, but not obvious in Group 5. It shows that in Group 5 of pollution degrees, the impact component at the time of 4.3 s is attenuated, indicating that 4.3 s is a characteristic moment of the fifth group of pollution degrees. The pollution degree of Group 3 and Group 5 has obvious impact components around 7.5 s and 8.0 s, respectively, indicating that Group 3 and Group 5 were significantly enhanced at these two moments. Around 8.7 s, there is a significant impact component in the pollution degree of Group 1. As the pollution level increases, the impact component is slowly attenuated. At around 9.8 s, there is a significant impact component in the pollution degree of Group 2. As the pollution level increases, the impact component of Group 3-5 is also gradually attenuated.

In the IMF 4 component, 0.1 s, 0.5 s, 0.8 s, and 2.7 s are the character moments of the pollution degree of Group 1, Group 2, Group 4, and Group 5, respectively. In the IMF 5 component, 8.7 s is the characteristic of Group 1. 0.6 s, and 9.8 s are the characteristics of Group 2. 7.5 s, 8.0 s, and 0.2 s are the characteristics of Group 3. Group 4 and 5. Their characteristics are mainly reflected in that the impact

components generated have been significantly enhanced during these times. In the IMF 4 component, 4.8 s and 9.5 s are the characteristics of Group3 and 4, while 6.7 s and 7.0 s are the characteristics of Group 5. In the IMF 5 component, 4.3 s is the characteristic of Group 5, and its characteristic is mainly manifested that the impact component generated has a significant weakening during these times. While in 2.1 s, 2.3 s, 3.0 s, 3.8 s, 6.4 s, 7.4 s, 8.1 s, and 8.5 s, the impact components of the IMF 4 components are more balanced under the pollution degree of each group. Secondly, in the IMF 4 component, the five groups of oils have obvious impact components at 3.0 s, 2.1 s, 4.6 s, 3.0 s, and 3.1 s. At the same time, there are obvious impact components at about 2 times, such as 6.1 s, 4.3 s, 9.0 s, 5.7 s, and 6.1 s, which shows that the impact component may be the group of contaminated oil Characteristic frequency.

IMF amplitude-frequency diagram

The Fourier transform is used to analyze the IMF components of each group of pollution signals, and the amplitude-frequency diagram shown in Fig. 5 is obtained, in which the vertical axis represents the signal amplitude, and the horizontal axis represents the frequency.

It can be seen from Fig. 5 that the frequency components of the five groups of IMF 1 components are the same as the original signal. Each IMF component has a more obvious approximately symmetrical small wave on both sides of the peak of its main frequency component, which indicates the pollution degree of each group. The frequency of the oil has obvious frequency modulation characteristics. In Fig. 5 (a), there are two frequencies with larger amplitudes of 20.22 Hz and 28.99 Hz in the IMF 2 component amplitude-frequency diagram. The frequency of the maximum amplitude in the IMF 3 component amplitude-frequency diagram is 20.29 Hz. There are four frequencies with larger amplitude in the IMF 4 amplitude-frequency diagram, which are 10.22 Hz, 11.44 Hz, 13.12 Hz, and 15.18 Hz, respectively. The frequency with the larger amplitude in IMF 5 is 4.96 Hz. In Fig. 5 (b), the frequencies with larger amplitudes in the IMF 2 component amplitude-frequency diagram are 15.72 Hz, 19.91 Hz, and 23.50 Hz, respectively. In IMF 3, there are two frequencies with a relatively large amplitude of 10.22 Hz and 13.66 Hz. There are 6 frequencies with large amplitude in IMF 4, namely 8.16 Hz, 8.84 Hz, 9.23 Hz, 11.60Hz, 12.28 Hz, and 12.82 Hz. The frequency with a larger amplitude in IMF 5 is 5.03 Hz. In Fig. 5 (c), the frequencies with larger amplitude in the IMF 2 component are 19.83 Hz, 22.66 Hz, and 27.92 Hz. The frequencies with a larger amplitude in IMF 3 are 13.27 Hz and 16.48 Hz. The frequency is 6.94 Hz. In Fig. 5 (d), the frequencies with larger amplitudes in the IMF 2 component are 15.49 Hz, 17.09 Hz, 18.77 Hz, 22.50 Hz, and 23.34 Hz, respectively. The frequency with the largest amplitude in the IMF 4 component is still 17.01 Hz, and its amplitude is 0.24×10^{-3} smaller than that of IMF 3. At the same time, the amplitudes at 10.22 Hz, 11.06 Hz, and 15.33 Hz are also larger. In Fig. 5 (e), the frequencies with the largest amplitudes of the IMF 2-4 components are 35.17 Hz, 16.48 Hz, and 9.46 Hz, respectively. In the IMF 2 and IMF 3 components, when the pollution degree changes from Group 2 to Group 5, the frequency with a larger amplitude tends to increase. In IMF 4-7, as the pollution degree increases, the frequency with a larger amplitude has certain fluctuations. The frequency with a larger amplitude increases first and then decreases, while in IMF4-7, with the increase of pollution degree, the frequency with a larger amplitude fluctuates to some extent. This is consistent with the conclusion that oil pulsation amplitude changes periodically with the increase of particle concentration at the same time in Fig. 4.

In order to better analyze the relationship between the five groups of pollution degrees and further extract the characteristic frequency, the IMF 2-7 components of the five groups of pollution degrees were collected and analyzed, as shown in Fig. 6. It can be found that each IMF component will have a large peak frequency at a basic interval of about 5.00 Hz, especially the IMF 2 and IMF 3 components are most obvious. Therefore, the frequency components in each IMF component are divided into frequency intervals with 5.00 Hz as a frequency segment.

It can be seen from Fig. 6 (a) that in the IMF 2 component, except for Group 3, the frequency components of the other groups are mainly distributed between 10.00-35.00 Hz, so we focus on analyzing the frequency in the range of 10.00-35.00 Hz. Around 10.00-15.00 Hz, as the pollution degree increases, the frequency in this interval tends to shift towards 15.00 Hz. Around 15.00-20.00 Hz, as the pollution degree increases, the frequency with a larger amplitude in this interval is slowly shifting toward 15.00-18.00 Hz. Around 20.00-25.00 Hz, as the pollution

(a) Group 1 contamination oil

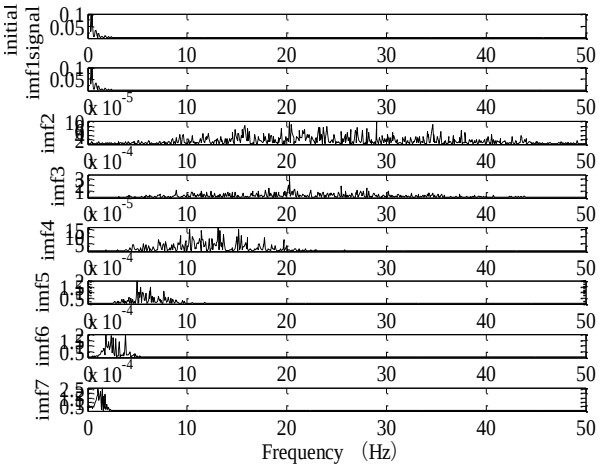

(b) Group 2 contamination oil

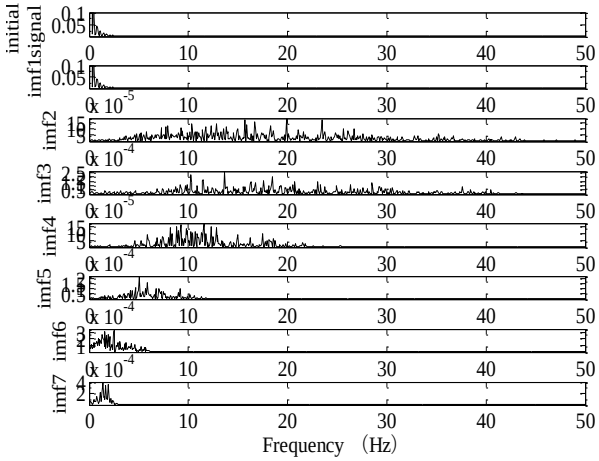

(c) Group 3 contamination oil

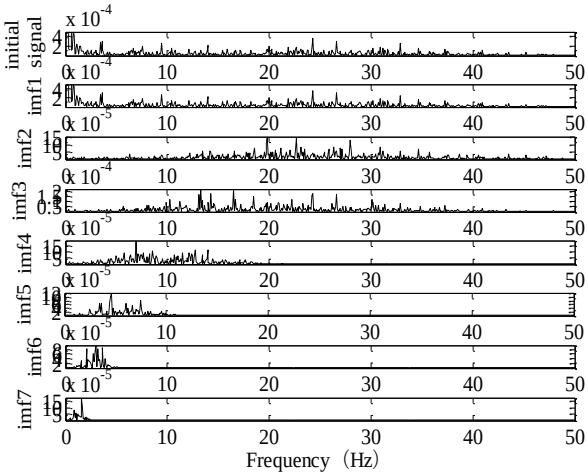

(d) Group 4 contamination oil

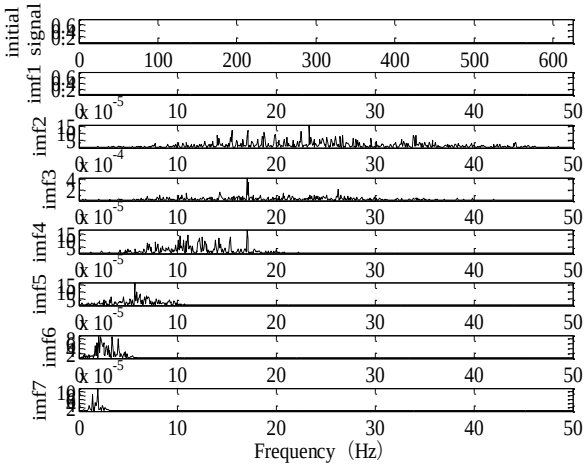

(e) Group 5 contamination oil

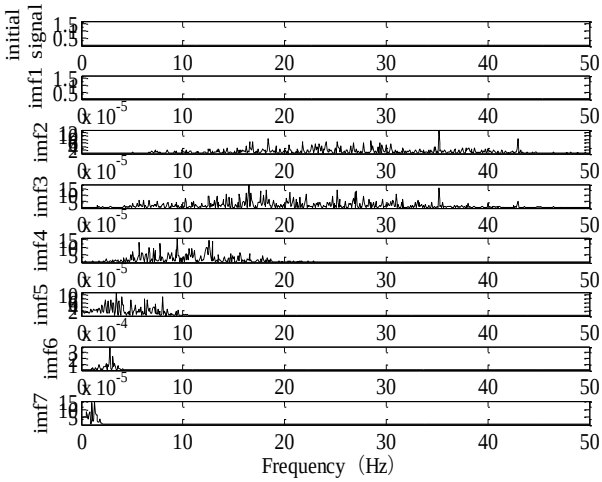

Fig. 5. Amplitude-frequency diagram of IMF components of oil signals with different pollution degrees.

degree increases, the oil frequency in this interval slowly shifts towards 21.00-23.00 Hz. Around 25.00-30.00 Hz, as the pollution degree increases, the frequency in this interval slowly shifts towards 26.00-28.00 Hz. Around 30.00-35.00 Hz, as the pollution degree increases, the oil frequency shifts towards 35.00 Hz. In Fig. 6 (b), about 10.00-15.00 Hz, as the pollution degree increases, the peak frequency around 15-20 Hz gradually shifts toward 17.00 Hz. Around 20.00-25.00 Hz, with the increase of the pollution degree, the frequency of the oil develops towards 25.00 Hz. Around 25.00-30.00 Hz, with the increase of the pollution degree, the frequency of the oil develops toward 26.00 Hz, and its frequency has been enhanced in the oil. Around 30.00-35.00 Hz, the pollution degree increases, and the oil frequency shifts towards 35.00 Hz. In Fig. 6 (c), about 5.00-10.00 Hz, the pollution degree increases, and the frequency in this interval gradually shifts forward. The pollution degree increases around 10.00-15.00 Hz, and the oil frequency shifts towards the middle of the interval. Around 15.00-20.00 Hz, the pollution degree increases, and the oil frequency gradually shift toward 15.00-17.00 Hz. In Fig. 6 (d), the five groups of pollution levels all have peak frequencies around 5 Hz, 4.96 Hz, 5.03 Hz, 4.57 Hz, 5.64 Hz, and 4.88 Hz, respectively. This shows that the pollution degree is increasing, and the low-frequency part of the oil is slowly developing towards 5.00 Hz; In Figs. 6 (e) and (f), the frequencies of IMF 6 and IMF 7 are mainly concentrated in 0-5.00 Hz. In IMF 6, as the pollution degree increases, the frequency of the oil gradually shifts toward 1 Hz, and the frequencies with larger amplitudes among the five groups of pollution degrees are around 1.60 Hz.

Secondly, among the six components, the amplitudes of IMF 3, IMF 6, and IMF 7 components are the largest, indicating that these three components are the main components of the oil signal. In the IMF 3 component, Group 1 has a maximum peak at 20.29 Hz, with an amplitude of 3.70×10^{-4}. In contrast, in the pollution degree of the 2-5 groups, there is no obvious peak frequency around 20.00 Hz, indicating 20.29 Hz is the characteristic frequency of Group 1 pollution degree. Group 2 has a maximum peak of 13.66 Hz, and the secondary peak frequency is 10.22 Hz, with an amplitude of 2.25×10^{-4}. At 10.22 Hz, the amplitude of the remaining groups at frequencies around 10.00 Hz is not obvious, but Group 3 is the secondary peak at 13.27 Hz, which is like the amplitude of Group 2. This shows that 10.22 Hz is the characteristic frequency of Group 3 of pollution degrees. Group 4 has the maximum peak frequency at 17.01 Hz, with an amplitude of 4.28×10^{-4}, while Group 1 at frequencies around 17.00 Hz is not obvious. Secondly, although Group 2, Group 3, and Group 5 have obvious peak frequencies around 17.00 Hz, their maximum amplitude is still about half that of Group 4, which shows that 17.01 Hz is the fourth Characteristic frequency. The characteristic frequencies of Groups 3 and 5 are not obvious in IMF 3. The characteristic frequencies of Groups 3 and 5 are not obvious in IMF 3, and the maximum peak frequencies of each pollution degree in IMF 5-7 components are around 5.00 Hz, 3.00 Hz, and 1.50 Hz, respectively, and the difference is not obvious. In the IMF 2 component, Group 2 has a significant peak frequency of around 5.00-10.00 Hz, while the other groups have no obvious peak frequency of around 5.00-10.00 Hz. In this interval, the maximum peak frequency of Group 2 is 10.38 Hz, and it can also be explained that 10.22 Hz is the characteristic frequency of the pollution degree of Group 2. Simultaneously, Group 5 has the maximum peak frequency at 35.17 Hz, with an amplitude of 1.32×10^{-4}. In comparison, the other groups have relatively small amplitudes at frequencies around 35.00 Hz, indicating that 35.17 Hz is characteristic of Group 5 frequency. Among the IMF 4 components, Group 3 has a maximum peak at 6.94 Hz with an amplitude of 1.99×10^{-4}. Although the other four groups have peaked around 6.00 Hz, the amplitudes are all less than 1×10^{-4}, which is not obvious relative to the amplitude of 6.94 Hz in Group 3. This shows that 6.94 Hz is the characteristic frequency of Group 3 of pollution degrees.

In summary, in the IMF 2- 4 component, the oil frequency shifts in the intermediate direction of the interval as the pollution degree increases. In the IMF 5-7 component, the frequency of the oil is mainly shifted in the direction of 5.00 Hz, 3.00 Hz, and 1.60 Hz, respectively. Secondly, the characteristic frequencies of 1-5 groups of polluted oils are 20.29 Hz, 10.22 Hz, 6.94 Hz, 17.01 Hz, and 35.17 Hz, respectively. This is because the oil in the test pipe section, under the action of the rotation frequency pulsation of the main shaft of the system, passes through the sudden expansion of the pipeline and forms a vortex structure leading to turbulence. Because of the Komanda effect, the asymmetric jet flow in the pipeline is deflecting, which leads to continuous stable, unstable and

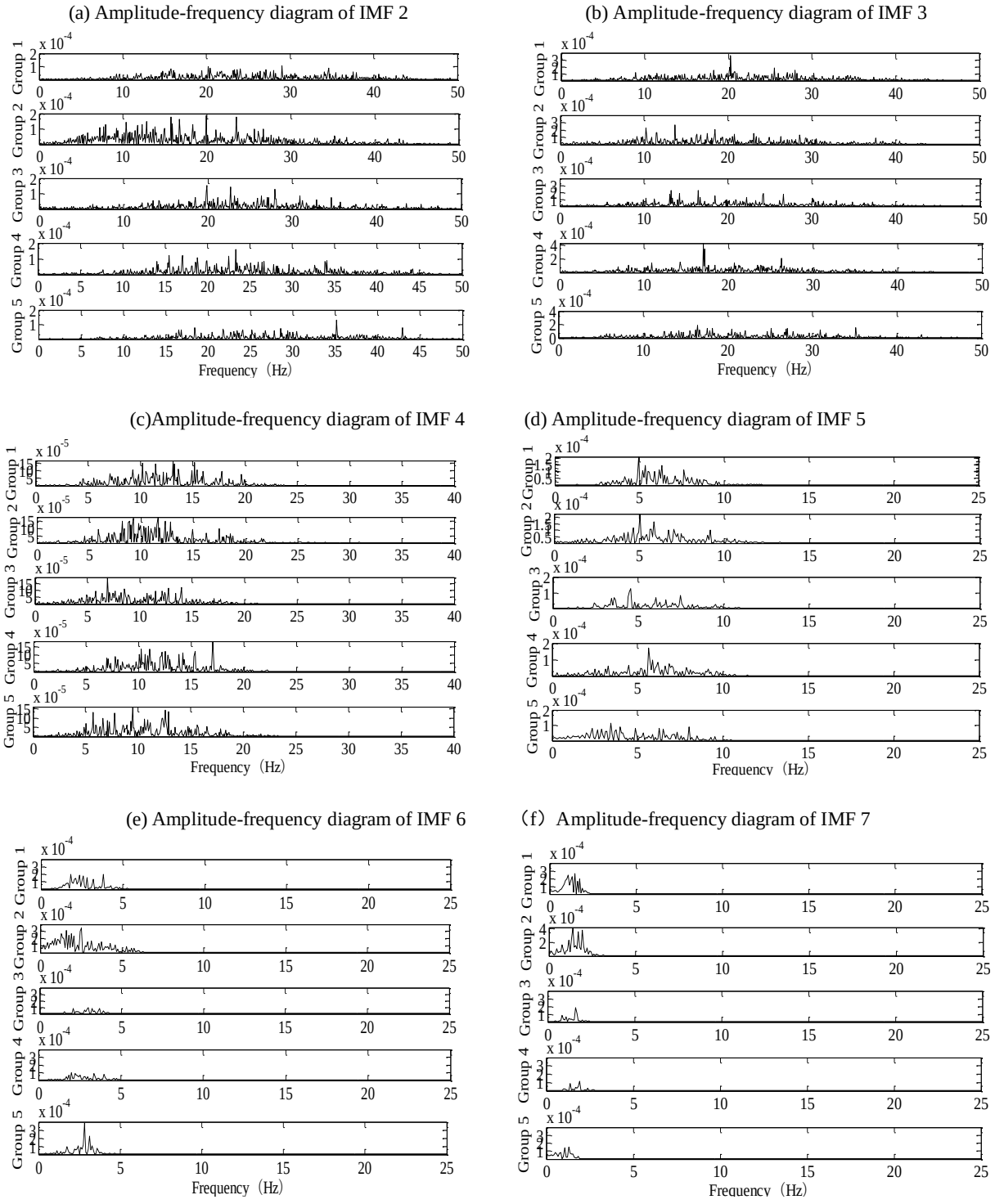

Fig. 6. Amplitude-frequency diagram of IMF 2-7 components.

turbulent flow of the oil and makes the pressure pulsation of the oil show obvious periodicity [23]. Due to the influence of the particles in the oil, this periodicity is accompanied by the increase of the particle concentration. When the particle concentration is lower than a certain number, the viscous shear force of the oil increases, thus reducing the pulsation degree of the oil. When the particle concentration exceeds this concentration, the settling

effect of particles makes the pipe wall form a rough wall, it enhances the turbulence burst behavior in the near-wall area, which leads to the increase of oil pulsation.

Through the collection and extraction of the experimental data of the motion state of contaminated oil in the pipeline, the differential pressure signals of oil with different contamination degrees were processed and analyzed by using the HHT method. The characteristic frequencies of oil signals with different contamination degrees were obtained according to the characteristic analysis of IMF components of each oil sample. Through the research of IMF frequency maps of oil signals with different pollution degrees, it is found that each IMF component has obvious frequency modulation characteristics under different pollution degrees. Based on the analysis of the Hilbert time spectrum of signal with different pollution degrees, the influence law of the natural frequency of oil in pipeline operation on the motion state of oil samples is obtained. It provides a preliminary research basis for further exploring the internal relationship between oil signals and oil pollution degree of different pollution degrees.

CONCLUSIONS

Due to the pressure signal of oil being time-varying and complicated, especially the pulsation of oil with a certain particle concentration is a typical non-stationary nonlinear signal, the traditional linear analysis method is not suitable for the analysis of oil signal. However, the Hilbert-Huang transform method is a new processing technology; it is not limited by Fourier analysis, and can carry out adaptive decomposition from the characteristics of the signal itself, and can describe the time spectrum and amplitude spectrum of the signal. Therefore, the HHT method was used to deal with the non-stationary nonlinear signal of oil pressure with particle concentration, to study the signal characteristics of oils with different pollution degrees in the pipeline. First, through the analysis of the IMF components of the five different groups of oil signals of different pollution degrees, the characteristics of the pollution levels of 0.1 s, 0.5 s, 0.8 s, and 2.7 s are Groups 1, 2, 4, and 5, respectively in the IMF 4 components; In the IMF 5 component, 8.7 s is the characteristic of Group 1 pollution degree. 0.6 s and 9.8 s are the characteristics of Group 2 pollution degrees. 7.6 s, 8.0 s, and 0.2 s are the characteristics of Group 3, Group 4, and Group 5, respectively. Their common characteristic is mainly reflected in the significant increase in the impact component generated during these times. Among the IMF 4 components, 4.8 s and 9.5 s are the characteristics of the pollution degree of Groups 3 and 4, respectively, and 6.7 s and 7.0 s are the characteristics of the pollution degree of Group 5. In the IMF 5 component, 4.3 s is characteristic of Group 5 pollution degree. Their common characteristic is mainly manifested in that the impact components generated have significantly weakened during these times. Second, by analyzing the IMF amplitude and frequency maps of the oil signals of 5 groups of different pollution degrees, it is obtained that under different pollution degrees, each IMF component has obvious frequency modulation characteristics. Simultaneously, as the pollution degree increases, the oil frequency of the IMF 2-4 component mainly shifts toward the middle of the interval, and the oil frequency of the IMF 5-7 component mainly shifts toward the direction of 5.00 Hz, 3.00 Hz, and 1.60 Hz. Secondly, the characteristic frequencies of the pollution levels in groups 1-5 are 20.29 Hz, 10.22 Hz, 6.94 Hz, 17.01 Hz, and 6.81 Hz, respectively.

The above research results show that HHT can obtain the characteristic values of oil pressure with different particle concentrations according to IMF energy, divide the frequency bands of oil pressure according to IMF component frequency characteristics, and take the energy of each frequency band as the characteristic value. The dynamic change of oil pressure with particle concentration is characterized by the energy change of the frequency band, which provides technical support for mastering the dynamic characteristics of particle pollution in oil operations.

Acknowledgments

This study was funded by Local science and technology development fund projects guided by the central government (206Z5201G), Chongqing Basic Research and Frontier Exploration Project (cstc2018jcyjAX0121), Fundamental Research Funds for the Central Universities (3142019001, 3142019055).

Received : Sep. 3, 2021 ; Accepted : Nov. 29, 2021

REFERENCES

[1] Lin J.H., Chang K.C., Particle Dispersion Simulation in Turbulent Flow Due to Particle-Particle and Particle-Wall Collisions, *Journal of Mechanics*, **32(02)**: 237-244(2016).

[2] Habib K.A., Cano D.L., Heredia J.A., Vicente-Escuder Á., Effect of Debris Size on the Tribological Performance of Thermally Sprayed Coatings, *Tribology International*, **143**: 106025(2020).

[3] Wang Z.-N., Kang Y., Li D., Wang X.-C., Hu D., Investigating the Hydrodynamics of Airlift Pumps by Wavelet Packet Transform and the Recurrence Plot, *Experimental Thermal and Fluid Science: International Journal of Experimental Heat Transfer, Thermodynamics, and Fluid Mechanics*, **92**: 56-68 (2018).

[4] Zhu Q., Liu Y., Hu H., Hou L., Guan M., Using Wavelet Denoising in Automatic Online Efficiency Estimation of a Hydraulic Excavator, *Transactions of the Institute of Measurement and Control*, **39(8)**: 1262-1270 (2017).

[5] Kalogerakou M.E., Maniatakis Ch.A., Spyrakos Ch.C., Psarropoulos P.N., Seismic Response of Liquid-Containing Tanks with Emphasis on the Hydrodynamic Response and Near-Fault Phenomena - Sciencedirect, *Engineering Structures*, **153**: 383-403(2017).

[6] Dan H.A, Sc B., Xl A., Wavelet Packet Analysis of Blasting Vibration Signal of Mountain Tunnel, *Soil Dynamics and Earthquake Engineering*, **117**: 72-80 (2019).

[7] Yan W., Tan J.W., Universiy Q.T., Fault Diagnosis of Rolling Bearing Based on Wavelet Packet Decomposition and EMD, *Coal Mine Machinery*, **36(2)**: 270-272 (2015).

[8] Hao Y., Sun Y., Jian L, Zhoumo Z., Variational Mode Decomposition and Probability Density Estimation of Lubricating Oil Debris Detection Signal, *Chinese Journal of Scientific Instrument*, **39(4)**: 99-106 (2018).

[9] Liang H.W., Zou D.F., Gao B.K., Kan L.L., Application of VMD Combined with Error Energy Algorithm in Pipeline Leakage Detection, *Control and Instruments in Chemical Industry*, **44(12)**: 1110-1113 (2017).

[10] Yuan-Bo X.U., Cai Z.Y., Application of Variational Modal Decomposition and K-L Divergence to Bearing Fault Diagnosis of Vibrating Screens, *Noise and Vibration Control*, **37(4)**: 160-165(2017).

[11] Yang Z., Johnson M., Hybrid particle Image Velocimetry with the Combination of Cross-Correlation and Optical Flow Method, *Journal of Visualization*, **20(3)**: 625-638 (2017).

[12] Wang D., Zhang Y., Jin B., Wang Y., Zhang M., Quasi-Distributed Optical Fiber Sensor for Liquid-Level Measurement, *IEEE Photonics Journal*, **9(6)**: 6805107(2017).

[13] Sumarna S., Purwanto A., Agustika D.K., Frequency Component Extraction of Heartbeat Cues with Short Time Fourier Transform (STFT), *J. Sains Dasar*, **5(1)**: 1-6 (2016).

[14] Meng L., Li Y., Wang W., Fu J., *Journal of Loss Prevention in the Process Industries*, **25(1)**: 90-102 (2012).

[15] Xu H., Yuan S., LI Z. "Analysis of the Time-Frequency Characteristics of Internal Combustion Engine Vibration Signal Based on Hilbert-Huang Transform", *2010 3rd International Congress on Image and Signal Processing*[C], YanTai, (2010).

[16] Qiu G., Ye J., Wang H., Investigation of Gas-Solids Flow Characteristics in a Circulating Fluidized Bed with Annular Combustion Chamber by Pressure Measurements and CPFD simulation, *Chemical Engineering Science*, **134**: 433-447 (2015).

[17] Fang P.M., Response of a Dual Triangulate Bluff Body Vortex Flowmeter to Oscillatory Flow, *Flow Measurement and Instrumentation*, **(35)**: 16-27 (2014).

[18] Ji H., Long J., Fu Y, Huang Z., Wang B., Li H., Flow Pattern Identification Based on EMD and LS-SVM for Gas–Liquid Two-Phase Flow in a Minichannel, *IEEE Transactions on Instrumentation & Measurement*, **60(5)**: 1917-1924 (2011).

[19] Li W.L., Zhong W.Q., Jin B.S., Xiao R., He T.-T., Flow Regime Identification in a Three-Phase Bubble Column Based on Statistical, Hurst, Hilbert–Huang Transform and Shannon Entropy Analysis, *Chemical Engineering Science*, **102**: 474-485(2013).

[20] Lu P., Han D., Jiang R., Chen X., Zhao Ch., Zhang G., Experimental Study on Flow Patterns of High-Pressure Gas–Solid Flow and Hilbert–Huang Transform Based Analysis, *Experimental Thermal and Fluid Science (EXP Term Fluid SCI)*, **51**: 174-182(2013).

[21] Li X., Liang S., Wang W., et al, Identification of Gas-liquid Two-phase Flow Patterns in Automobile Hydraulic Braking Systems, *Zhongguo Jixie Gongcheng/China Mechanical Engineering*, **28(4)**: 492-496(2017).

[22] Li J., Wang H., Liu Z, Chen Sh., Zheng Ch., An Experimental Study on Turbulence Modification in the Near-Wall Boundary Layer of a Dilute Gas-Particle Channel Flow, *Experiments in Fluids*, **53(5)**: 1385-1403(2012).

[23] Vétel J., Garon A., Pelletier D., et al, Asymmetry and Transition to Turbulence in a Smooth Axisymmetric Constriction, *Journal of Fluid Mechanics*, **607**: 351-386 (2008).